Journal of Nanophotonics

Nanophotonics.SPIEDigitalLibrary.org

Femtosecond spectroscopy on MoS_2 flakes from liquid exfoliation: surfactant independent exciton dynamics

Daniele Vella
Victor Vega-Mayoral
Christoph Gadermaier
Natasa Vujicic
Tetiana Borzda
Peter Topolovsek
Matej Prijatelj
Iacopo Tempra
Eva A. A. Pogna
Giulio Cerullo

SPIE.

Femtosecond spectroscopy on MoS_2 flakes from liquid exfoliation: surfactant independent exciton dynamics

Daniele Vella,[a,b,*] Victor Vega-Mayoral,[a,b] Christoph Gadermaier,[a,b,*] Natasa Vujicic,[a,c] Tetiana Borzda,[a,b] Peter Topolovsek,[a,b,d] Matej Prijatelj,[a,b] Iacopo Tempra,[e] Eva A. A. Pogna,[e] and Giulio Cerullo[e]

[a]Jožef Stefan Institute, Department of Complex Matter, Jamova 39, Ljubljana 1000, Slovenia
[b]Jožef Stefan International Postgraduate School, Jamova 39, Ljubljana 1000, Slovenia
[c]Institute of Physics, Bijenicka 46, Zagreb 10000, Croatia
[d]Italian Institute of Technology, Center for Nano Science and Technology, Via Pascoli 70/3, Milan 20133, Italy
[e]Politecnico di Milano, IFN-CNR, Department of Physics, P. Leonardo da Vinci 32, Milan 20133, Italy

Abstract. Ionic surfactants, which are widely used to stabilize nanomaterials in dispersions, can drastically alter the nanomaterial's photophysical properties. Here, we use femtosecond optical spectroscopy to study the dynamics of excitons and charges in few-layer flakes of the two-dimensional semiconductor MoS_2. We compare samples obtained via exfoliation in water with different amounts of adsorbed sodium cholate, obtained by repeated washing of the dried flakes. We find that the femtosecond dynamics is remarkably stable against the surfactant adsorption, with a slight increase of the initial exciton quenching occurring during the first few picoseconds as the only appreciable effect. [DOI: 10.1117/1.JNP.10.012508]

Keywords: MoS_2; two-dimensional crystals; transition metal dichalcogenides; femtosecond spectroscopy; ionic surfactants.

Paper 15079SS received Aug. 6, 2015; accepted for publication Sep. 16, 2015; published online Nov. 5, 2015.

1 Introduction

In the last five years, most of the know-how acquired by the carbon community and culminating in the discovery and exploitation of graphene[1] has been transferred to isolate and engineer transition metal dichalcogenide (TMD) layered materials. Semiconducting TMDs, such as MoS_2, WS_2, $MoSe_2$, and WSe_2, can also be exfoliated into two-dimensional (2-D) layers of single unit cell thickness, suitable for logic devices and optoelectronics applications.[2–4] A peculiarity of the semiconducting TMDs is the crossover from indirect to direct gap semiconductor when going from bulk or few-layer material to monolayers.[5] This is a result of the gradual change of the band structure as a function of the number of layers due to quantum confinement.[6]

Liquid exfoliation has been proven to produce stable dispersions of flakes of 2-D TMDs via a procedure that involves ultrasonication and centrifugation. However, processing nanomaterials in liquid dispersion can crucially alter their optical response and their electronic properties.[7] For example, during continuous wave excitation of single wall carbon nanotubes (SWNTs) covered with sodium cholate, chemisorption of oxygen leads to hole doping and photoluminescence quenching. In low pH solution, protonation of the oxygen absorbed on an SWNT with a sodium dodecyl sulfate shell bleaches the optical absorption and consequently quenches the luminescence by Auger recombination.[8–10] Moreover, it localizes electrons on the SWNT and increases the number of holes in the valence band (VB).[11] The surfactant surrounding SWNT can induce

*Address all correspondence to: Daniele Vella, E-mail: daniele.vella@ijs.si; Christoph Gadermaier, E-mail: christoph.gadermaier@ijs.si

photoluminescence blinking via trapping photoexcited charges followed by a slow recombination. This process also changes the emission spectrum via Stark effect.[12,13]

Femtosecond pump-probe spectroscopy represents a versatile technique to study the electron dynamics in semiconducting nanomaterials. It has elucidated, for instance, the dynamics of charge carriers, excitons, and phonons[14,15] or the Stark effect induced by photogenerated and trapped charge carriers.[16] Here, we use femtosecond pump-probe spectroscopy to study few-layer MoS_2 from liquid exfoliation in water and sodium cholate[17] with different amounts of adsorbed surfactant controlled by a multistep washing protocol. We exploit the sensitivity of the pump-probe signal to the change of the electronic excited state population[18] in order to investigate the effect of the surfactant on the carrier and exciton dynamics of MoS_2. For different amounts of surfactant, we obtain the same shape and relaxation behavior of the pump-probe spectra. This work demonstrates the optical stability of MoS_2 against surfactant adsorption, which sets it apart from other semiconducting nanomaterials.

2 Experimental Details

2.1 *Sample Preparation*

An initial solution of 4.5 g sodium cholate and 15 g of MoS_2 in powder form (Sigma Aldrich) dissolved in 1 l of deionized (DI) water was ultrasonicated for 100 h, using an Elmasonic P ultrasonic bath at 37 kHz and maximum power. This solution, which contains the flakes of MoS_2, was used as a starting point for producing all the samples.[4]

In order to obtain films of few-layer MoS_2 flakes with high surfactant content (SC), 10 ml of ethanol was added to 10 ml of the main solution, which was then spray-deposited on a quartz substrate (kept at 150°C). In parallel, different washing steps have been done to produce samples with medium and low SC.

MoS_2 with medium SC was obtained by centrifugation of a part of the initial solution in a Cole Parmer Power Spin BX centrifuge for 60 min at 11,000 rpm, followed by the addition of clean DI water and ultrasonication in a bath. This procedure was repeated three times to remove a part of the surfactant from the solution and from the MoS_2 surface. At a later stage, ethanol was added as described above, and the mixture was sprayed on quartz. Figure 1(a) shows a transmission electron microscope image of a typical few-layer MoS_2 flake obtained by this process. To further reduce the concentration of sodium cholate on the surface of MoS_2, we introduced an additional step in the procedure for the medium SC samples: after each centrifugation, the solution was washed with DI water and HCl (0.1 ml of 1 M HCl per 50 ml of MoS_2 dispersion). HCl reacts with sodium cholate and forms sodium chloride and cholic acid, which is soluble in ethanol. This step is expected to remove most of the sodium cholate from the flake surface. Such obtained low SC dispersion is again deposited on a quartz substrate.

As a reference sample, we used MoS_2 obtained in crystalline form (Wolfram Camp Mining Ltd.), expanded in hydrazine[19] and exfoliated, without surfactant, in the organic solvent N-methyl-2-pyrrolidone by ultrasonication. The films were deposited on quartz substrates by a Langmuir-Blodgett process.[20]

2.2 *Pump-Probe Spectroscopy*

The laser source was a commercial regeneratively amplified mode-locked Ti:sapphire laser (Coherent Libra), yielding pulses at 1 kHz repetition rate, with 800 nm center wavelength and 100 fs duration. The pump pulses were generated by frequency doubling the fundamental in a thin β barium borate crystal. The pump energy was 140 nJ energy per pulse, with 150 μm spot size. Broadband white-light continuum pulses generated in a sapphire plate, covering the 420 to 750 nm wavelength range, were used as probe pulses. The pump and probe beams were polarized parallel to each other. After passing through the sample, the probe beam was focused onto the entrance slit of a spectrometer equipped with a 1024-pixel back-thinned CCD sensor S7030-1006 and electronics specially designed for fast read-out times and low noise.[21] By recording the transmitted probe spectrum with (T_{on}) and without (T_{off}) the pump as a function

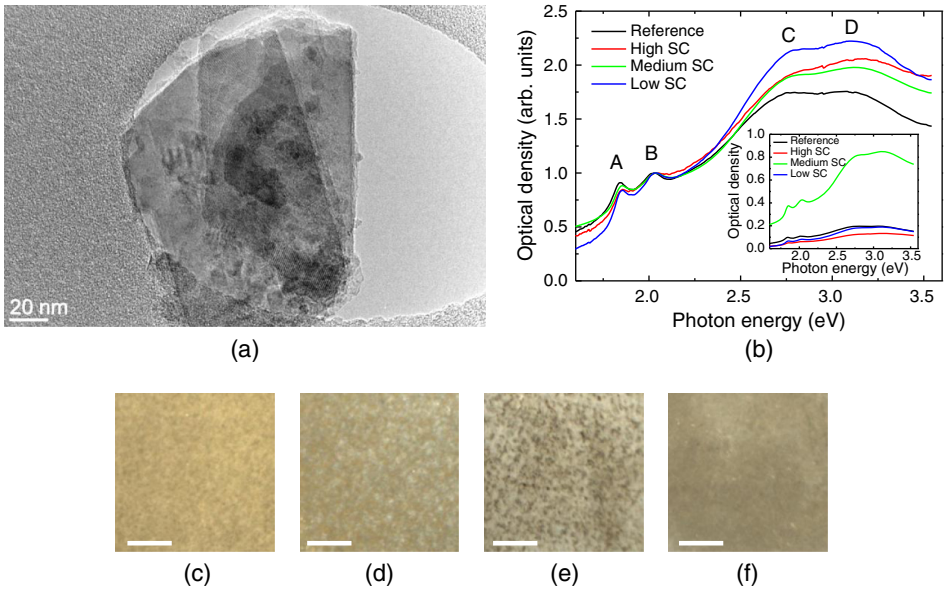

Fig. 1 (a) Transmission electron microscope image of few layers of MoS_2 from liquid exfoliation in deionized water and sodium cholate. (b) Absorption spectra of few-layer MoS_2 ensembles from liquid exfoliation with different surfactant content (SC) and a reference sample exfoliated via a surfactant-free process normalized to the B-exciton resonance. Inset shows actual optical density. Bright-field mages from an optical microscope of MoS_2 deposited on a quartz substrate: (c) low SC, (d) medium SC, (e) high SC, and (f) reference. Scale bar: 1 mm.

of wavelength λ and pump-probe delay τ, we obtain the differential transmission ($\Delta T/T$) spectrum as

$$\Delta T/T(\lambda,\tau) = [T_{\text{on}}(\lambda,\tau) - T_{\text{off}}(\lambda,\tau)]/T_{\text{off}}(\lambda,\tau). \quad (1)$$

The delay between pump and probe pulse was varied by moving a translation stage, which changes the length of the optical path of one beam with respect to the other.

2.3 *Absorption Spectroscopy*

The optical absorption spectra were recorded in transmission using a V-570 Jasco spectrometer with 0.5 nm spectral resolution, equipped with a single monochromator covering the spectral range from 190 to 2500 nm (6.52 to 0.49 eV).

2.4 *Raman Spectroscopy*

Raman spectroscopy of MoS_2 was performed with an NT-MDT NTEGRA SPECTRA confocal Raman microscope in backscattering geometry with spectral resolution of 0.7 cm^{-1}. We used the excitation line at 488 nm and a 20× objective (N.A. 0.4) to focus onto a spot size of 20 μm. The Raman signals were detected with a CCD array at −80°C. We used a laser power of 5 mW.

3 Results and Discussion

The normalized absorption spectra in Fig. 1(b) show the characteristic exciton resonances A to D at 1.8, 2.0, 2.8, and 3.0 eV. The resonances A and B are ascribed to excitons associated with the direct gap transition at the K point.[22,23] The splitting originates primarily from the splitting of the VB due to spin-orbit coupling. The C exciton is ascribed either to a transition from a band below the VB toward the conduction band (CB) or to a transition from the VB into a nested region[24] of the CB. The D exciton is commonly ascribed to impurities.[22]

Recently, it has been shown that for surfactant dispersions of MoS_2, the characteristics of the absorption spectrum provide a metric for the average flake size and thickness.[25] Since it has been formally proven only for aqueous dispersion, we do not extract any quantitative characterization from our absorption spectra; however, the general trends should be valid also for dried films. Specifically, the ratio between the B exciton peak and the absorption at 3.6 eV is a measure of the typical flake size, and the position of the A exciton peak is a measure of the typical flake thickness (number of layers). The samples differ very little in both respects, the most significant difference being that the reference sample, probably due to the different exfoliation protocol, seems to consist of somewhat smaller flakes. Repeated washing, on the other hand, does not appreciably affect the flake size and thickness distribution.

To evaluate the homogeneity of the films on the relevant scale of 150 microns (the spot size used for the pump-probe experiment), we show optical images of the deposited MoS_2 [Figs. 1(c)–1(f)]. The darker hue of green seen for the medium SC film, matched by a higher optical density and stronger Raman and pump-probe signals (see below), is due to a higher film thickness. For the used high concentration, our simple spraying technique gives little control over the spraying speed and hence the film thickness. A significant inhomogeneity is seen only for the high SC sample. The high surfactant concentration may favor lateral aggregation of flakes or have an influence on the drying dynamics of the film. However, the apparent islands and voids are small enough to mostly average out over the spot size of the pump-probe experiment.

To find out whether the inhomogeneity in the film thickness is also related to an inhomogeneity in the flake characteristics, we measured Raman spectra (depicted in Fig. 2) on each sample on four randomly selected spots with a distance of several millimeters and a spot size of 20 microns, much smaller than the characteristic length scale of the inhomogeneity. The distance between the peaks E^1_{2g} (in-plane mode) and A_{1g} (out-of-plane mode) is a robust measure of the flake thickness.[26] We obtain $\Delta\omega = 24.5\ \mathrm{cm}^{-1}$, corresponding to an average flake thickness of four layers for the high SC sample, and $\Delta\omega = 25\ \mathrm{cm}^{-1}$, corresponding to five or more layers for all the others.

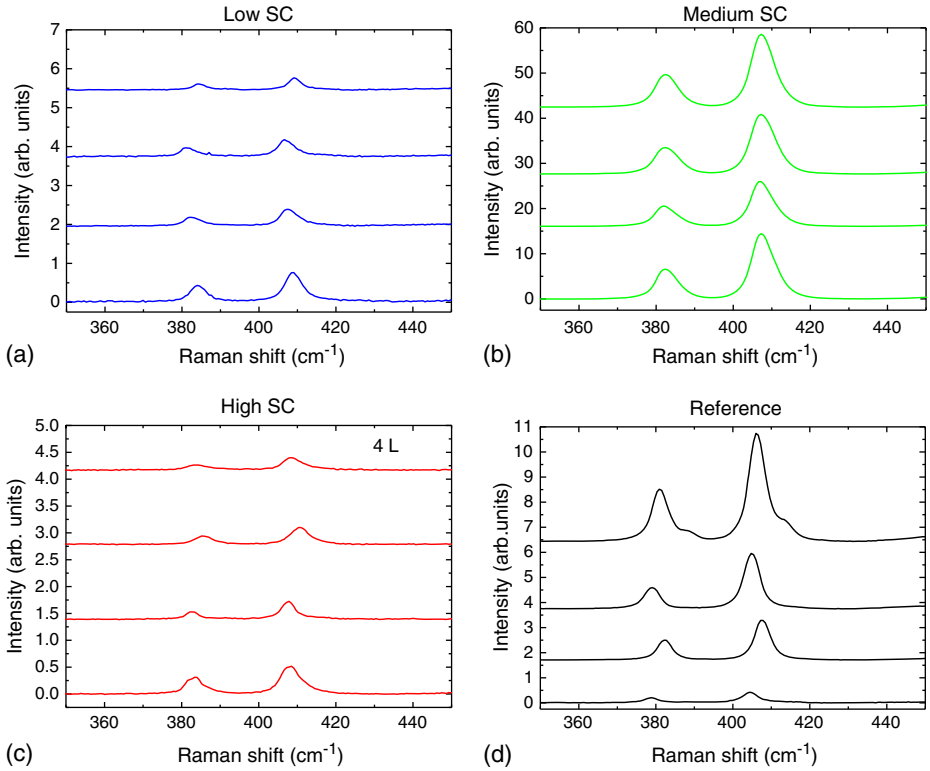

Fig. 2 Raman spectra for excitation at 488 nm in four different points of the sample: (a) low SC, (b) medium SC, (c) high SC, and (d) reference.

Given the similar electronic structure of the flakes within the same film, we can use the Raman intensity as an indication of the amount of material present.[27] The thicker sample (medium SC) shows a similar Raman intensity at all spots, while for the others, the intensity varies strongly. This confirms the observation in the optical micrographs that on a length scale of 20 microns, the thicker sample is quite homogeneous, while the others are not. However, the flake thickness and hence the electronic structure is more homogeneous, and over the spot size of the pump-probe experiment (150 microns), the inhomogeneity averages out.

The $\Delta T/T$ spectra of the reference sample are shown in Fig. 3(a) for different pump-probe delays. As previously observed on MoS_2, there are six salient features in the visible spectral range:[28] three photobleaching peaks of the exciton absorption resonances A^0, B^0, and C^0, and three photoinduced absorption peaks A^-, B^-, and C^- ascribed to photogenerated charges,

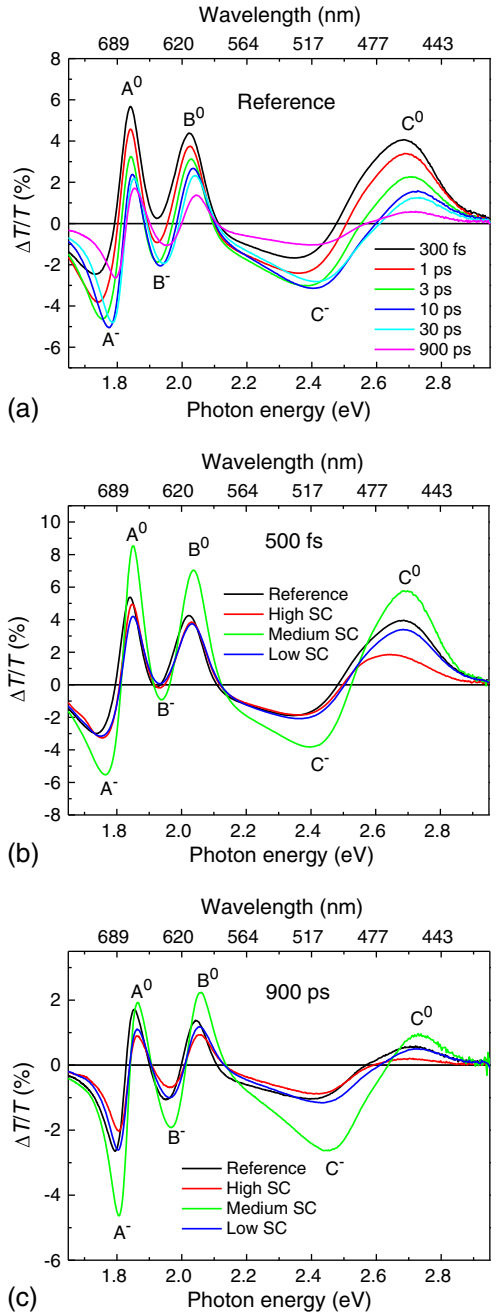

Fig. 3 (a) $\Delta T/T$ spectra of the reference sample at selected pump-probe delays. Comparison of $\Delta T/T$ spectra at (b) 500 fs and (c) 900 ps pump-probe delays for different samples.

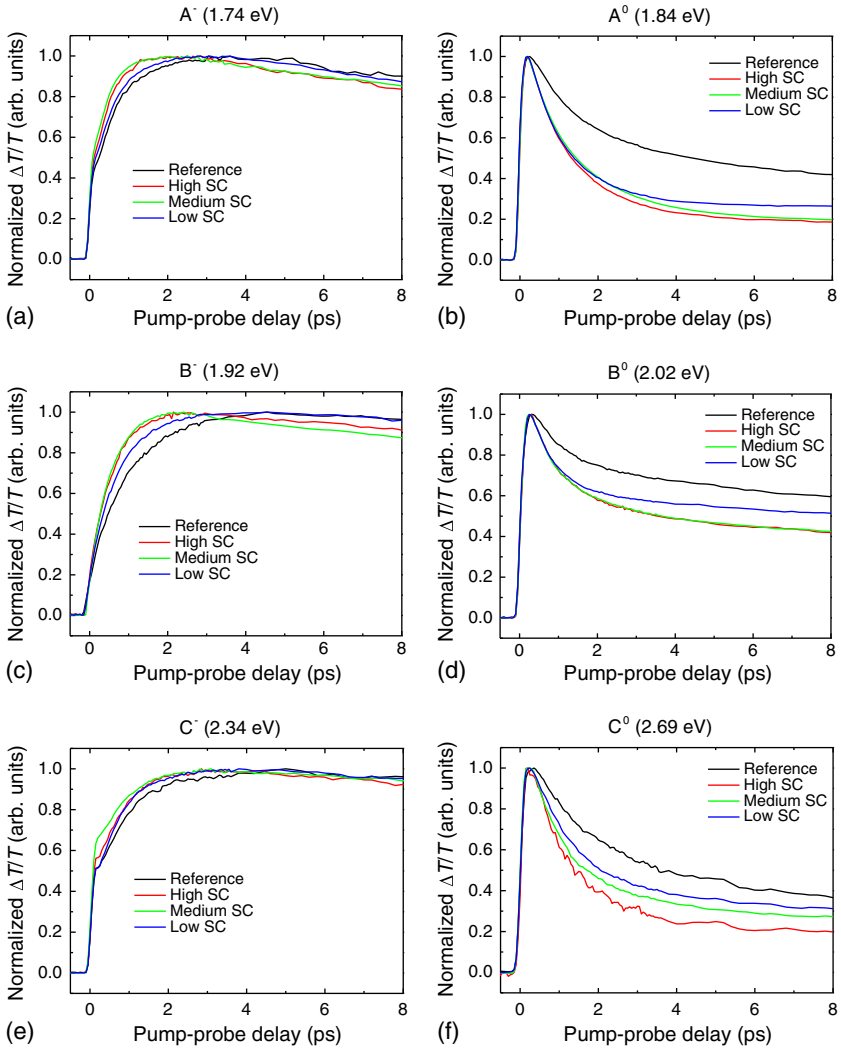

Fig. 4 $\Delta T/T$ dynamics for different samples at selected probe energies: (a) 1.74, (b) 1.84, (c) 1.92, (d) 2.02, (e) 2.34, and (f) 2.69 eV.

one for each of the excitons. The exciton bleaching features show a fast decay during the first few picoseconds, followed by a slower decay on the few-100 ps scale. The photoinduced absorption peaks grow during the first few picoseconds and then decay with a characteristic time similar to the slow exciton decay. Charge photogeneration occurs via a combination of a direct excitation mechanism (i.e., within our instrumental resolution of ~100 fs), and via dissociation of hot excitons, on a time scale of a few hundred femtoseconds to few picoseconds.[28] This process can be seen in Fig. 3(a) as a fast decrease of the bleaching features A^0, B^0, and C^0 and a corresponding growth of the charge features A^-, B^-, and C^- during the first few picoseconds. Together with the spectral change of shape—relative increase of the absorption and decrease of the bleaching features—the peaks also undergo a blueshift with increasing delay. In a more comprehensive study with different excitation fluences, it was found that the more the excited states the more the spectra are shifted to the red.[28] This has been explained as Stark effect due to photoexcited charges,[16,29] inter-excitonic interaction,[30] or band gap renormalization.[31] Additionally, at short delays, the A^- and C^- photoinduced absorption peaks appear artificially redshifted due to the strong overlap with the A^0 and C^0 bleaching peaks, respectively. The fast decay of the bleaching peaks diminishes this effect with increasing pump-probe delay, resulting in an additional apparent temporal blueshift of these two photoinduced absorption features. After ~10 ps, there is no significant shift of the spectra anymore and all features decay with a time constant of several hundred picoseconds, as has already been observed[14] on individual flakes of MoS_2. Comparing the reference sample with those of different SC [Figs. 3(b) and 3(c)],

one finds a trend toward slightly faster decay for higher SC. Additionally, for higher SC, the C exciton bleaching is weaker.

The trend toward faster initial exciton decay for higher SC observed in the $\Delta T/T$ spectra is confirmed by the dynamics at representative probe energies, close to the respective spectral peaks depicted in Figs. 4(a)–4(f). The timescale of the delayed charge formation [Figs. 4(a), 4(c), and 4(e)] corresponds to that of the initial exciton decay [Figs. 4(b), 4(d), and 4(f)], confirming the origin of these charges from the dissociation of excitons. Both the slow (few hundred picoseconds) decay component as well as the direct and delayed charge photogeneration yields do not vary appreciably between the different samples.

In conclusion, we have shown that the exciton and charge dynamics in few-layer MoS_2 flakes is robust against adsorption of the anionic surfactant sodium cholate. This is in stark contrast to other nanomaterials such as carbon nanotubes[32] or C_{60} fullerenes,[33] where anionic surfactants generally lead to strong exciton quenching. This robustness highlights the viability of surfactant-assisted liquid processing (exfoliation, deposition, printing, etc) of MoS_2 and other semiconducting TMDs.

Acknowledgments

D.V., V.V.-M., T.B., N.V., I.T., and E.A.A.P. performed the experiments under the guidance of G. C. P.T. and M.P. prepared the samples. D.V. and C.G. analyzed the data and wrote the paper with critical input from all authors. We appreciate the stimulating discussions with J. Strle. The research leading to these results has received funding from LASERLAB-EUROPE (grant agreement no. 284464, EC's Seventh Framework Programme), the Marie-Curie ITN "MoWSeS," the ERC Advanced Grant "Trajectory," the Graphene Flagship (contract no. CNECT-ICT-604391), and the Center of Excellence in Nanoscience and Nanotechnology, Slovenia. The research was carried out in the context of the COST "Nanospectroscopy."

References

1. K. S. Novoselov et al., "Two-dimensional atomic crystals," *Proc. Nat. Acad. Sci.* **102**, 10451–10453 (2005).
2. Q. H. Wang et al., "Electronics and optoelectronics of two-dimensional transition metal dichalcogenides," *Nat. Nanotech.* **7**, 699–712 (2012).
3. B. Radisavljevic et al., "Single-layer MoS_2 transistors," *Nat. Nanotech.* **6**, 147–150 (2011).
4. J. N. Coleman et al., "Two-dimensional nanosheets produced by liquid exfoliation of layered materials," *Science* **331**, 568–571 (2011).
5. K. F. Mak et al., "Atomically thin MoS_2: a new direct-gap semiconductor," *Phys. Rev. Lett.* **105**, 136805 (2010).
6. A. Splendiani et al., "Emerging photoluminescence in monolayer MoS_2," *Nano Lett.* **10**, 1271–1275 (2010).
7. E. A. Obraztsova et al., "Effect of environment on ultrafast photoexcitation kinetics in single-wall carbon nanotubes," *Phys. Status Solidi B* **247**, 2831–2834 (2010).
8. F. Wang et al., "Observation of rapid Auger recombination in optically excited semiconducting carbon nanotubes," *Phys. Rev. B* **70**, 241403 (2004).
9. A. L. Efros and M. Rosen, "Random telegraph signal in the photoluminescence intensity of a single quantum dot," *Phys. Rev. Lett.* **78**, 1110–1113 (1997).
10. P. A. Frantsuzov and R. A. Marcus, "Explanation of quantum dot blinking without the long-lived trap hypothesis," *Phys. Rev. B* **72**, 155321 (2005).
11. M. S. Strano et al., "Reversible, band-gap-selective protonation of single-walled carbon nanotubes in solution," *J. Phys. Chem. B* **107**, 6979–6985 (2003).
12. O. Kiowski et al., "Single-walled carbon nanotubes show stable emission and simple photoluminescence spectra with weak excitation sidebands at cryogenic temperatures," *Phys. Rev. B* **76**, 075422 (2007).
13. K. Matsuda et al., "Photoluminescence intermittency in an individual single-walled carbon nanotube at room temperature," *Appl. Phys. Lett.* **86**, 123116 (2005).
14. H. Shi et al., "Exciton dynamics in suspended monolayer and few-layer MoS_2 crystals," *ACS Nano* **7**, 1072–1080 (2013).

15. T. Koyama et al., "Transient absorption kinetics associated with higher exciton states in semiconducting single-walled carbon nanotubes: relaxation of excitons and phonons," *J. Phys. Chem. C* **117**, 20289–20299 (2013).
16. G. Soavi et al., "Ultrafast charge photogeneration in semiconducting carbon nanotubes," *J. Phys. Chem. C* **117**, 10849–10855 (2013).
17. R. J. Smith et al., "Large-scale exfoliation of inorganic layered compounds in aqueous surfactant solutions," *Adv. Mater.* **23**, 3944–3948 (2011).
18. J. Cabanillas-Gonzalez, G. Grancini, and G. Lanzani, "Pump-probe spectroscopy in organic semiconductors: monitoring fundamental processes of relevance in optoelectronics," *Adv. Mater.* **23**, 5468–5485 (2011).
19. J. Zheng et al., "High yield exfoliation of two-dimensional chalcogenides using sodium naphthalenide," *Nat. Commun.* **5**, 2995 (2014).
20. W. M. R. Divigalpitiya, R. F. Frindt, and S. R. Morrison, "Thin oriented films of molybdenum disulfide," *Thin Solid Films* **186**, 177–192 (1990).
21. D. Polli, L. Lüer, and G. Cerullo, "High-time-resolution pump-probe system with broadband detection for the study of time-domain vibrational dynamics," *Rev. Sci. Instrum.* **78**, 103108 (2007).
22. R. F. Frindt and A. D. Yoffe, "Physical properties of layer structures: optical properties and photoconductivity of thin crystals of molybdenum disulphide," *Proc. R. Soc. A* **273**, 69–83 (1963).
23. D. Y. Qiu, F. H. da Jornada, and S. G. Louie, "Optical spectrum of MoS_2: many-body effects and diversity of exciton states," *Phys. Rev. Lett.* **111**, 216805 (2013).
24. D. Kozawa et al., "Photocarrier relaxation pathway in two-dimensional semiconducting transition metal dichalcogenides," *Nat. Commun.* **5**, 4543 (2014).
25. C. Backes et al., "Edge and confinement effects allow in situ measurement of size and thickness of liquid-exfoliated nanosheets," *Nat. Commun.* **5**, 4576 (2014).
26. H. Li et al., "From bulk to monolayer MoS_2: evolution of Raman scattering," *Adv. Funct. Mater.* **22**, 1385–1390 (2012).
27. C. Lee et al., "Anomalous lattice vibrations of single- and few-layer MoS_2," *ACS Nano* **4**, 2695–2700 (2010).
28. T. Borzda et al., "Charge photogeneration in few-layer MoS_2," *Adv. Funct. Mater.* **25**, 3351–3358 (2015).
29. C. Gadermaier et al., "Long lived charged states in single-walled carbon nanotubes," *Nano Lett.* **6**, 301–305 (2006).
30. S. Sim et al., "Exciton dynamics in atomically thin MoS_2: interexcitonic interaction and broadening kinetics," *Phys. Rev. B* **88**, 075434 (2013).
31. G. Tränkle et al., "General relation between band gap renormalization and carrier density in two-dimensional electron-hole plasmas," *Phys. Rev. B* **36**, 6712–6714 (1987).
32. C. Georgi et al., "Photoinduced luminescence blinking and bleaching in individual single-walled carbon nanotubes," *Chem. Phys. Chem.* **9**, 1460–1464 (2008).
33. A. F. Clements et al., "Photophysical properties of C_{60} colloids suspended in water with Triton X-100 surfactant: excited-state properties with femtosecond resolution," *J. Phys. Chem. A* **113**, 6437–6445 (2009).

Daniele Vella received his MSc degree in biomedical engineering from the University of Pisa in 2013. In October 2013, he joined the Department of Complex Matter at the Jozef Stefan Institute (JSI), Slovenia, as a PhD student. His research interests include optical and electronic properties of nanomaterials with specific attention to femtosecond spectroscopy on thin films and devices based on two-dimensional semiconducting transition metal dichalcogenides.

Christoph Gadermaier has studied applied physics and, after two years as visiting scientist at the Politecnico di Milano, Italy, obtained his PhD in 2002 from Graz University of Technology, Austria, on ultrafast photoexcitation dynamics in conjugated polymers. After two years as a postdoc at the Politecnico di Milano and two years at JSI, Slovenia, he became research associate at JSI and associate professor at the JSI International Post-Graduate School.

Biographies for the other authors are not available.